1

Unclassified
SECURITY CLASSIFICATION OF THIS PAGE

REPORT DOCUMENTATION PAGE

Form Approved
OMB No. 0704-0188

AD-A232 004

1b. RESTRICTIVE MARKINGS

3. DISTRIBUTION/AVAILABILITY OF REPORT
Approved for public release; Distribution unlimited

4. PERFORMING ORGANIZATION REPORT NUMBER(S)
PL-TR-91-2030

5. MONITORING ORGANIZATION REPORT NUMBER(S)

6a. NAME OF PERFORMING ORGANIZATION
Phillips Lab, Geophysics Directorate

6b. OFFICE SYMBOL (If applicable)
OPS

7a. NAME OF MONITORING ORGANIZATION

6c. ADDRESS (City, State, and ZIP Code)
Hanscom AFB
Massachusetts 01731-5000

7b. ADDRESS (City, State, and ZIP Code)

DTIC
ELECTE
MAR 11 1991
S G D

8a. NAME OF FUNDING/SPONSORING ORGANIZATION

8b. OFFICE SYMBOL (If applicable)

9. PROCUREMENT INSTRUMENT IDENTIFICATION NUMBER

8c. ADDRESS (City, State, and ZIP Code)

10. SOURCE OF FUNDING NUMBERS

PROGRAM ELEMENT NO	PROJECT NO	TASK NO	WORK UNIT ACCESSION NO
63220C	S321	13	01

11. TITLE (Include Security Classification)
Impulse Formalism for Atom-diatom Collisions

12. PERSONAL AUTHOR(S)
Ramesh D. Sharma, Pradip M. Bakshi*, Joseph M. Sindoni**

13a. TYPE OF REPORT	13b. TIME COVERED	14. DATE OF REPORT (Year, Month, Day)	15. PAGE COUNT
Reprint	FROM _____ TO _____	1991 February 14	15

16. SUPPLEMENTARY NOTATION *Physics Department, Boston College, Chestnut Hill MA 02167
**Yap Analytics Inc., 594 Marrett Road, Lexington, MA 02173 - Reprinted from Physical Review A, Volume 43, Number 1, 1 January 1991

17. COSATI CODES			18. SUBJECT TERMS (Continue on reverse if necessary and identify by block number)
FIELD	GROUP	SUB-GROUP	*Atom; *Molecule; Impulse; Cross-sections; Collisions

19. ABSTRACT (Continue on reverse if necessary and identify by block number)

An exact formulation of the impulse approach (IA), or quantum-mechanical spectator model, is applied to atom-diatom collisions. Results are compared with previous work on the IA, which has always involved the peaking approximation (PA). The PA is seen to overestimate (underestimate) differential cross sections for processes involving projectile atom energy loss (gain). The internal consistency of the IA is explored by subjecting it to semidetailed balancing. For small scattering angles the IA is seen to be an inadequate theory, probably due to the neglect of double- and higher-collision terms in the multiple-collision expansion of the three-body T matrix. For large scattering angles, where the IA does appear to describe the scattering process accurately, the exact calculation is shown to give the same results as when only the energy-conserving on-the-energy-shell two-body processes are considered. An accurate approximation method is also developed for rapid computation of inelastic differential cross sections. Finally, the calculated results are compared with the experimental measurements, and the need to explore two-body potentials more complicated than the hard-core potential is pointed out.

20. DISTRIBUTION/AVAILABILITY OF ABSTRACT
☐ UNCLASSIFIED/UNLIMITED ☒ SAME AS RPT. ☐ DTIC USERS

21. ABSTRACT SECURITY CLASSIFICATION
Unclassified

22a. NAME OF RESPONSIBLE INDIVIDUAL	22b. TELEPHONE (Include Area Code)	22c. OFFICE SYMBOL
Ramesh D. Sharma	(617) 377-4198	OPS

DD Form 1473, JUN 86 *Previous editions are obsolete.* SECURITY CLASSIFICATION OF THIS PAGE
Unclassified

PL-TR-91-2030

PHYSICAL REVIEW A VOLUME 43, NUMBER 1 1 JANUARY 1991

Impulse formalism for atom-diatom collisions

Ramesh D. Sharma
Optical/Infrared Technology Division, Geophysics Laboratory, Hanscom Air Force Base, Massachusetts 01731

Pradip M. Bakshi
Physics Department, Boston College, Chestnut Hill, Massachusetts 02167

Joseph M. Sindoni
Yap Analytics Inc., 594 Marrett Road, Lexington, Massachusetts 02173

(Received 15 June 1990)

An exact formulation of the impulse approach (IA), or quantum-mechanical spectator model, is applied to atom-diatom collisions. Results are compared with previous work on the IA, which has always involved the peaking approximation (PA). The PA is seen to overestimate (underestimate) differential cross sections for processes involving projectile atom energy loss (gain). The internal consistency of the IA is explored by subjecting it to semidetailed balancing. For small scattering angles the IA is seen to be an inadequate theory, probably due to the neglect of double- and higher-collision terms in the multiple-collision expansion of the three-body T matrix. For large scattering angles, where the IA does appear to describe the scattering process accurately, the exact calculation is shown to give the same results as when only the energy-conserving on-the-energy-shell two-body processes are considered. An accurate approximation method is also developed for rapid computation of inelastic differential cross sections. Finally, the calculated results are compared with the experimental measurements, and the need to explore two-body potentials more complicated than the hard-core potential is pointed out.

I. INTRODUCTION

The basic idea of the impulse approach to analyzing collisions was proposed by Chew[1] in his study of inelastic scattering of high-energy neutrons by deuterons. When the time duration of the collision is much shorter than the period of characteristic motion of the bound particle, the components of the bound particle may be considered to act independently of each other, with position or momentum amplitudes given by the bound-state wave function. The binding potential only serves to create a relative momentum distribution of target particles. The three-body scattering amplitude thus reduces to an appropriately weighted sum of two-body scattering amplitudes. The constituent not taking part in the scattering process is called the spectator. The impulse approach has therefore also become known as the quantum-mechanical spectator model. The scattered state is obtained by combining the effects of the two two-body collisions with proper phase factors. The probability amplitude of a given final state is obtained by projecting the scattered state onto it. It should be emphasized that the perturbation of the initial state is not assumed small; the only assumption is that the two scattering centers act suddenly, and therefore independently. Formal development of Chew's work has been provided by Chew and Wick,[2] Ashkin and Wick,[3] and Chew and Goldberger.[4] The impulse approach has been discussed in texts by Goldberger and Watson[5] and Rodberg and Thaler,[6] the latter giving a very readable account. The impulse approach (IA) has been applied to a number of situations in scattering theory. Coleman[7] has developed the IA with applications to electron-atom collisions and Korsch *et al.*[8] have developed the IA with applications to electron-molecule collisions. It has also been applied extensively in nuclear physics.[5]

The IA was first applied to atom-diatom collisions by Bogan[9] and by Eckelt, Korsch, and Philipp (EKP).[10] The latter authors in a series of papers[11-13] have applied the IA to a number of situations involving atom-diatom collisions. The IA has also been applied to atom-diatom collisions by Beard and Micha.[14] In the IA, the T matrix is expanded in a multiple-collision series[10] and only the terms representing single collisions are retained—two terms for an atom-diatom collision and so on. In addition, while not a part of the basic IA formalism, the atom-diatom calculations cited above use another approximation as well, namely the peaking approximation (PA), to obtain results for comparison with experiments. In the PA, (i) the t matrix representing the two-body process is evaluated at a particular value of the spectator atom momentum, and (ii) the slow variation of the t-matrix elements over a region of appreciable overlap of the initial and the final states is used to justify the separation of the three-body T-matrix elements into two parts—one containing information about dynamics (the two-body t matrix) and the other containing information about the target (the form factor). $T^{(3)}$ will be used to denote the three-body transition matrix while the two-body transition matrix will be denoted by $t^{(3)}$. The PA

gives a very nice physical picture of the impulse scattering process. However, it was recently shown by the present authors[15] that, except for elastic scattering, the PA results are substantially different from the exact IA calculation. We note here in passing that the PA was also found to be inadequate for the excitation of atomic hydrogen by 1–500-keV protons.[16]

In this paper we give, in detail, an exact formulation of the impulse calculation without invoking the PA. Also, as in past studies, the target molecule has been taken to be in a low state of internal excitation, and a large translational energy of relative motion is assumed to justify the use of the IA and the PA. It was pointed out by Sharma[17] that the IA can also be used in situations involving large internal excitation and small or moderate relative translational energies. Since our formalism does not invoke any special properties of the T matrix or the wave functions, the resulting equations are applicable for arbitrary internal molecular and relative kinetic energies. Section II formulates the problem, where we follow the methodology of Eckelt *et al.*[10] Section III derives the peaking approximation to relate the present work to the previous work and to set the stage for the exact calculation, which is derived in Sec. IV. Section V compares the exact results with the PA results. Section VI checks the internal consistency of the results obtained from the IA, using semidetailed balancing. Section VII gives an approximation for the scattering amplitude, which is easily computed, yet accurate. Section VIII compares the calculated results with the experimental measurements. Concluding remarks are given in Sec. IX.

II. FORMULATION

The differential cross section, in the center-of-mass system, for a rotational-vibrational transition is given by[10]

$$\frac{d\sigma}{d\Omega}(vjp_3 \rightarrow v'j'p_3';\theta) = \frac{p_3'}{(2j+1)p_3} \times \sum_m \sum_{m'} \left| \left[\frac{2\pi}{\hbar} \right]^2 \mu_3 \langle \phi_3' | T(E+i0) | \phi_3 \rangle \right|^2 , \quad (1)$$

where $|\phi_3\rangle \equiv |v,j,m,\mathbf{p}_3\rangle$ denotes the initial state, the final-state variables are denoted by primes, and $\mathbf{p}_3$ and $\mathbf{p}_3'$ are the momenta of the incident particle before and after the collision. $\mathbf{p}_3$ is also the momentum of the incident particle 3 with respect to the center of mass (c.m.) of the molecule 12. $\mathbf{p}_a$ denotes the momentum of particle a with respect to the c.m. of bc, and $\mathbf{q}_a$ is the relative momentum of b and c. This set of momenta is called the Jacobi momenta. μ_a denotes the reduced mass of the system (a,bc). θ is the scattering angle, i.e., the angle between $\mathbf{p}_3$ and $\mathbf{p}_3'$. The summation over m and m' has removed the dependence of the differential cross section on the azimuthal angle. $T(E+i0)$ is the three-body matrix element with total initial (or final) energy E. μ_{ab} is the reduced mass of the two particles a and b, and $M = m_1 + m_2 + m_3$.

In a coordinate system with the origin coincident with the c.m. of the three particles, only two momenta are independent, and any $\mathbf{p}$ or $\mathbf{q}$ may be expressed in terms of two other $\mathbf{p}$'s and/or $\mathbf{q}$'s. The vibrational-rotational energy of the molecule 12 will be expressed through $\mathbf{q}_3$, which will later be written in terms of $\mathbf{q}_1$ ($\mathbf{q}_2$) and $\mathbf{p}_1$ ($\mathbf{p}_2$) when atom 1 (2) is the spectator atom. The spectator-atom momentum remains constant during the collision. At the end of the collision $\mathbf{q}_3'$ is resynthesized from $\mathbf{q}_s'$ and the spectator momentum $\mathbf{p}_s' = \mathbf{p}_s$, $s = 1,2$. The probability amplitude of the final state is the projection of the state $\langle \mathbf{q}_3' |$ on the final state.

It has been pointed out that the validity of the impulse approach requires that the time duration of the collision be much shorter than the period of characteristic motion of the target. Previous work on inelastic atom-diatom scattering using the IA has assumed a hard-sphere or hard-core potential between the incident atom and either of the two atoms constituting the target. This potential satisfies the IA criterion for any internal or relative translational energy of motion. Another reason for using this model potential is that the required half-on-shell, as well as off-the-shell, two-body t-matrix elements are given in literature in a closed form. In this work, we will also use this potential. This will facilitate the comparison of our results with those of earlier workers. In addition, since our calculation is exact, we will be able to learn about the impulse approach itself. We are, however, aware that an infinitely steep potential overestimates highly nonresonant transitions. In subsequent work, we plan to explore this point by using less steep two-body potentials.

The potential energy of the three-body system V can be written as

$$V = V_{3M}(x,y,\alpha) + V_3(y) , \quad (2)$$

where V_{3M} is the interaction between incident atom 3 and the diatom M. x is the distance of the incident atom 3 from the c.m. of the molecule, y is the internuclear distance of the diatom, and α is the angle between x and y. V_3 is the potential energy of the diatom 12. To give a description of the three-body scattering process in terms of two-body scattering and a spectator atom requires that the interaction potential be written as

$$V_{3M} = V_1(y_1) + V_2(y_2) , \quad (3)$$

where $V_a \equiv V_{bc}$ and y_2 (y_1) is the distance between atom 1 (2) and atom 3,

$$y_1\ (y_2) = \{x^2 + [c_1\ (c_2)y]^2 \mp 2xyc_1\ (c_2)\cos\alpha\}^{1/2} , \quad (4)$$

with $c_1\ (c_2) \equiv m_2\ (m_1)/(m_1+m_2)$; the minus sign applies to subscript 1 and the plus sign applies to subscript 2. The form for the atom-molecule potential used in Eq. (3) does not give a good fit to the more common form of this potential in terms of Legendre polynomials. The two potentials are applicable to different models of atom-diatom collisions. It is desirable to establish a connection between the two models, and this will be attempted in a future work.

Following EKP,[10] we write the three-body T matrix in

the multiple-collision series

$$T=T^{(1)}+T^{(2)}+T^{(1)}G_3T^{(2)}+T^{(2)}G_3T^{(1)}+\cdots , \quad (5)$$

where the three-body transition matrix $T^{(s)}$, $s=1,2$, denotes the collision of atoms 3 and t, $t=2,1$, s being the spectator atom and $G_3=(z-H_0-V_3)^{-1}$ being the propagator or the Green's function (H_0 being the total kinetic-energy operator). Equation (3) has a simple physical interpretation. The first two terms denote the collision of atoms 32 and 31, respectively. The next two terms denote double collision ij, where 3 collides first with j and then with i, and so on. It should be stressed that this is not an expansion in the Born series, and each of the terms on the right-hand side of Eq. (5) represents a three-body T matrix. The IA keeps only the first two terms.

To reduce the three-body matrix $T^{(s)}$ into the two-body matrix $t^{(s)}$, one writes

$$T^{(1)}=V_1\Omega^{(1)} , \quad (6)$$

where the Møller operator $\Omega^{(1)}$ is defined by

$$\Omega^{(1)}=1+(z-H_0-V_3-V_1)^{-1}V_1 , \quad (7)$$

$V_1\equiv V_{23}$, the potential between atoms 2 and 3. The Møller operator in Eq. (7) is still a three-body operator. We now invoke the spirit of the IA, i.e., the time duration of the collisions is much shorter than periods of characteristic motion. This allows one to assume that the internuclear distance of the diatom stays constant during the collision and to replace the operator V_3, the potential energy between bound particles 1 and 2, by a number. Writing $z-V_3=z_{IA}$, we get the two-particle Møller operator Ω_1 describing the collision between particles 3 and 2,

$$\Omega_1=1+(z_{IA}-H_0-V_1)^{-1}V_1 . \quad (8)$$

In Eq. (7), $z=E_{VR}+E_{rel}+i0$, where E_{VR} is the vibrational-rotational energy of the diatomic molecule, and $E_{rel}=p_3^2/(2\mu_3)$ is the relative atom-diatom translational energy. Writing $E_{VR}-V_3=q_3^2/(2\mu_{12})$, where q_3 and μ_{12} are the relative momentum and reduced mass of atoms 1 and 2, respectively, we get

$$z_{IA}=p_3^2/(2\mu_3)+q_3^2/(2\mu_{12})+i0 . \quad (9)$$

z_{IA} is then the kinetic energy of the three particles in the center-of-mass system. z_{IA} are the eigenvalues of H_0, eigenfunctions being the free-particle states $|\phi_0\rangle$ described in the next paragraph. We have now translated into quantitative language the assertion of the IA that the role of the diatom potential is to generate a relative momentum distribution of its two constituent atoms. We should point out that there are other choices for z_{IA} that have been used in literature.[14,18]

The transition matrix elements between eigenstates ϕ_3 of H_0+V_3 can be written as

$$\langle\phi_3'|T^{(s)}|\phi_3\rangle=\sum_{\phi_0',\phi_0}{}'\sum\langle\phi_3'|\phi_0'\rangle\langle\phi_0'|t^{(s)}|\phi_0\rangle\langle\phi_0|\phi_3\rangle , \quad (10)$$

where the summation is over the initial and final free-particle states ϕ_0 and ϕ_0', and ϕ_3, as pointed out earlier, denotes $|\mathbf{p}_3\rangle=|\mathbf{p}_3\rangle\otimes|vjm\rangle$, etc. The above expression can be simplified by noting that $|\phi_0\rangle=|\mathbf{q}_3\rangle\otimes|\mathbf{p}_3\rangle$ provides a complete set for the free-particle momentum states,

$$\sum_{\phi_0}|\phi_0\rangle\langle\phi_0|\phi_3\rangle=\int|\mathbf{q}_3\mathbf{p}_3'\rangle\langle\mathbf{q}_3\mathbf{p}_3'|\phi_3\rangle d\mathbf{p}_3'd\mathbf{q}_3$$
$$=\int|\mathbf{q}_3\mathbf{p}_3\rangle\phi(\mathbf{q}_3)d\mathbf{q}_3 , \quad (11)$$

with the molecular wave function in the momentum representation given by

$$\langle\mathbf{q}_3|\phi_3\rangle\equiv\phi(\mathbf{q}_3)$$
$$=(2\pi)^{-3/2}\int d\mathbf{r}\exp(i\mathbf{q}_3\cdot\mathbf{r})\langle\mathbf{r}|vjm\rangle$$
$$=(2/\pi)^{1/2}i^jI_{vj}(q_3)Y_{jm}(\hat{q}_3) . \quad (12)$$

Y_{jm} are the spherical harmonics and I_{vj} is defined by

$$I_{vj}(q_3)=\int_0^\infty dr\,r^2\chi_{vj}(r)j_j(q_3r) , \quad (13)$$

$\chi_{vj}(r)$ being the radial part of the vibration-rotation wave function and j_j representing the spherical Bessel function of order j. Similarly,

$$\sum_{\phi_0'}{}'\langle\phi_3'|\phi_0'\rangle\langle\phi_0'|=\int\phi^{*'}(\mathbf{q}_3')d\mathbf{q}_3'\langle\mathbf{q}_3'\mathbf{p}_3'| , \quad (14)$$

where $\phi'(\mathbf{q}_3')$ is the final molecular state. Using Eqs. (11) and (14) we can write Eq. (10) as

$$\langle\phi_3'|T^{(s)}|\phi_3\rangle=\int\phi^{*'}(\mathbf{q}_3')\langle\mathbf{q}_3'\mathbf{p}_3'|t^{(s)}|\mathbf{q}_3\mathbf{p}_3\rangle$$
$$\times\phi(\mathbf{q}_3)d\mathbf{q}_3d\mathbf{q}_3' . \quad (15)$$

To calculate the matrix elements of the two-body transition operator $t^{(s)}$, it is pertinent to recall that the spectator Jacobi momentum $\mathbf{p}_s$ stays constant during the collision, and momenta $\mathbf{p}_3$ and $\mathbf{q}_3$ must be expressed in terms of $\mathbf{p}_s$ and $\mathbf{q}_s$, $s=1,2$. $\mathbf{q}_s$ is changed to $\mathbf{q}_s'$ during the collision and, after the collision, inverse transformation to $\mathbf{p}_3'$ and $\mathbf{q}_3'$ is carried out. These transformations are effected by the relations

$$\mathbf{q}_3=-\{\mathbf{p}_1+[m_1/(m_1+m_2)]\mathbf{p}_3\} , \quad (16)$$

$$\mathbf{q}_3=\{\mathbf{p}_2+[m_2/(m_1+m_2)]\mathbf{p}_3\} , \quad (17)$$

$$\mathbf{q}_1=[m_3/(m_2+m_3)]\mathbf{p}_1+\mathbf{p}_3 , \quad (18)$$

and,

$$\mathbf{q}_2=-\{[m_3/(m_1+m_3)]\mathbf{p}_2+\mathbf{p}_3\} . \quad (19)$$

Equations (16) and (18) are used when atom 1 is the spectator, while Eqs. (17) and (19) are used when atom 2 is the spectator. Expressions for $\mathbf{q}_k'$ are obtained from Eqs. (16)–(19) by replacing $\mathbf{p}_k$ by $\mathbf{p}_k'$. In a three-atom system,

with the origin at the center of mass, we have $\mathbf{p}_1+\mathbf{p}_2+\mathbf{p}_3=0$, and only two momenta are independent. This choice of momenta greatly simplifies the solution.

Noting that the state $|\mathbf{p}_3\mathbf{q}_3\rangle$ is also the state $|\mathbf{p}_s\mathbf{q}_s\rangle$, $s=1,2$ [Eqs. (16)–(19)], we are in a position to write

$$\langle \mathbf{q}'_3\mathbf{p}'_3|t^{(s)}|\mathbf{q}_3\mathbf{p}_3\rangle=\langle \mathbf{p}'_s|\mathbf{p}_s\rangle\langle \mathbf{q}'_s|t^{(s)}|\mathbf{q}_s\rangle$$
$$=\delta(\mathbf{p}'_s-\mathbf{p}_s)\langle \mathbf{q}'_s|t^{(s)}|\mathbf{q}_s\rangle\ , \tag{20}$$

where the basic assumption of the IA (namely that the spectator momentum remains constant during the collision) is reflected by the Dirac δ function. We can now rewrite Eq. (15) as

$$\langle \phi'_3|T^{(s)}|\phi_3\rangle=\int d\mathbf{q}'_3\delta(\mathbf{p}'_s-\mathbf{p}_s)d\mathbf{q}_3\phi^{*'}(\mathbf{q}'_3)$$
$$\times\langle \mathbf{q}'_s|t^{(s)}|\mathbf{q}_s\rangle\phi(\mathbf{q}_3)\ . \tag{21}$$

Changing the integration variable from $\mathbf{q}'_3$ to $\mathbf{p}'_s$, analogous to the transformation carried out in Eqs. (18) and (19), we get

$$\langle \phi'_3|T^{(s)}|\phi_3\rangle=\int d\mathbf{q}_3\phi^{*'}(\mathbf{q}'_3)\langle \mathbf{q}'_s|t^{(s)}|\mathbf{q}_s\rangle\phi(\mathbf{q}_3)\ . \tag{22}$$

Going back to Eq. (1), the expression for the differential scattering cross section can be written as

$$\frac{d\sigma}{d\Omega}(vjp_3\rightarrow v'j'p'_3,\theta)=\frac{p'_3}{p_3(2j+1)}\sum_m\sum_{m'}\left|\left(\frac{2\pi}{\hbar}\right)^2\mu_3\left\langle\phi'_3\left|\sum_{s=1,2}T^{(s)}\right|\phi_3\right\rangle\right|^2\ . \tag{23}$$

At this point we note a particular feature of the IA. It has been pointed out that q_s changes to q'_s during the collision between atoms 3 and t. This change of the magnitude of the relative momentum during scattering from a central field does not conserve energy during the two-body collisions. After the collision, only those combinations of p'_3 and internal molecular energy $(v'j')$ that conserve energy are permitted. This nonconservation of energy during the two-body collision should pose no problem, since the uncertainty in energy, ΔE, and time duration of the collision, Δt, are connected by the uncertainty relation $\Delta E\approx\hbar/\Delta t$. In an impulse collision with a hard-core potential, $\Delta t\rightarrow 0$. Therefore there is a large uncertainty in energy. This was the reason, as we pointed out earlier, that the hard-core potential probably overestimates highly nonresonant transitions. Energy associated with q_s is physical in the sense that $z_{1A}=q_s^2/(2\mu_{tu})+p_s^2/(2\mu_s)$, the kinetic energy of the three-body system in the c.m. frame, whereas the corresponding energy associated with $q'_s\neq q_s$ is not physical. For this reason, the two-body t-matrix elements $t^{(s)}(\mathbf{q}_s,\mathbf{q}'_s;z_{1A})$ are called half-on-the-energy-shell matrix elements. The use of momentum $\mathbf{q}'_s$, which does not conserve energy, has, as we have shown elsewhere,[18] interesting consequences for time-reversal (TR) symmetry. It should be pointed out that half-on-shell and off-shell matrix elements have also been interpreted as incomplete collisions.[19] The two-body t matrix discussed here does not describe the complete scattering process; it is therefore consistent with this interpretation.

III. THE PEAKING APPROXIMATION

The peaking approximation (PA) is based on the idea that the product of the initial and final state in Eq. (22) is nonzero in a finite region of the spectator momentum and the t matrix is slowly varying in this region. Thus we can evaluate the $t^{(s)}$ matrix element at some particular value of the momenta,

$$t^{(s)}_{\mathrm{PA}}=[\langle \mathbf{q}'_s|t^{(s)}|\mathbf{q}_s\rangle]_{\mathbf{p}_s=\mathbf{p}^0_s}\ , \tag{24}$$

where $\mathbf{q}_3$ and $\mathbf{p}_3$ are related by Eq. (16) or (17).

The spectator momentum at which the t matrix is evaluated is arrived at in the literature by the following argument: Since the momentum distributions at which initial- and final-state wave functions, $\phi_3(\mathbf{q}'_3)$ and $\phi'_3(\mathbf{q}'_3)$, are nonzero only in the vicinity of

$$\mathbf{q}_3=\mathbf{0}\rightarrow\mathbf{p}_s=-\frac{m_s}{(m_1+m_2)}\mathbf{p}_3\ , \tag{25}$$

and

$$\mathbf{q}'_3=\mathbf{0}\rightarrow\mathbf{p}_s=-\frac{m_s}{(m_1+m_2)}\mathbf{p}'_3\ , \tag{26}$$

the product of the wave functions is substantially different from zero only in the vicinity of their midpoint,

$$\mathbf{p}^0_s=-\frac{m_s}{2(m_1+m_2)}(\mathbf{p}_3+\mathbf{p}'_3)\ . \tag{27}$$

This argument holds strictly for the $v=0$ and the $j=0$ state of the molecule. If there is a large amount of energy in the vibration and/or rotation of the molecule, the wave function is no longer substantially different from zero only in the neighborhood of $\mathbf{q}_3=\mathbf{0}$ (or $\mathbf{q}'_3=\mathbf{0}$), and the PA may have to be evaluated at some other value of the spectator momentum.

Proceeding further, we can now rewrite Eq. (22) as

$$\langle \phi'_3|T^{(s)}|\phi_3\rangle=t^{(s)}_{\mathrm{PA}}\int d\mathbf{q}_3\phi^{*'}(\mathbf{q}'_3)\phi(\mathbf{q}_3)\ . \tag{28}$$

The integral in Eq. (28) is an overlap integral, describing the amplitude for the instantaneous transition from the initial to the final state, due to impulsive momentum increment,

$$\mathbf{q}_3\rightarrow\mathbf{q}'_3=\mathbf{q}_3+(-1)^s\frac{m_s}{(m_1+m_2)}\mathbf{q}\ , \tag{29}$$

$\mathbf{q}$ being the momentum transferred during the collision, $\mathbf{q}\equiv\mathbf{p}_3'-\mathbf{p}_3$. This integral is cast in familiar form and, at the same time, its evaluation is simplified by a transformation to coordinate space, leading to

$$\langle\phi_3'|T^{(s)}|\phi_3\rangle=t_{\mathrm{PA}}^{(s)}\int d\mathbf{r}\,\Psi^{*'}(\mathbf{r})\exp(-i\alpha_s\mathbf{q}\cdot\mathbf{r})\Psi(\mathbf{r})\ , \tag{30}$$

where

$$\alpha_s\equiv(-1)^s\frac{m_s}{(m_1+m_2)}\ . \tag{31}$$

Taking initial- and final-state wave functions as

$$\Psi(\mathbf{r})=\chi_{vj}(r)Y_{jm}(\hat{r}) \tag{32}$$

and

$$\Psi'(\mathbf{r})=\chi_{v'j'}(r)Y_{j'm'}(\hat{r})\ , \tag{33}$$

respectively, and using the expansion of the plane wave in spherical harmonics, we get

$$\langle\phi_3'|T^{(s)}|\phi_3\rangle=t_{\mathrm{PA}}^{(s)}4\pi\sum_{\lambda}\pm i^{\lambda}\left|\frac{\hat{j}\hat{\lambda}}{4\pi\hat{j}'}\right|^{1/2}C(j\lambda j';00)C(j\lambda j';m,\mu)f_{v'j',vj;\lambda}^{(s)}(q)Y_{\lambda\mu}^{*}(\hat{q})\ , \tag{34}$$

where $\mu\equiv m'-m$, the C's are the Clebsch-Gordan coefficients,[20] $\hat{j}\equiv(2j+1)$, etc., $\pm$ means that the plus sign is taken for $s=1$ and the minus sign for $s=2$, and

$$f_{v'j',vj;\lambda}^{(s)}\equiv\int_0^{\infty}dr\,r^2\chi_{v'j'}(r)j_{\lambda}(|\alpha_s|rq)\chi_{vj}(r\ . \tag{35}$$

The differential cross section is obtained by averaging over the initial azimuthal quantum numbers and summing over the final ones, giving

$$\frac{d\sigma}{d\Omega}(vjp_3\rightarrow v'j'p_3',\theta)=\left|\frac{2\pi}{\hbar}\right|^4\mu_3^2\frac{p_3'}{p_3}\sum_{\lambda=|j-j'|}^{\lambda=(j+j')}\hat{\lambda}C^2(j\lambda j';00)|f_{v'j',vj;\lambda}^{(1)}t_{\mathrm{PA}}^{(1)}+(-1)^{\Delta j}f_{v'j',vj;\lambda}^{(2)}t_{\mathrm{PA}}^{(2)}|^2\ , \tag{36}$$

an expression available in the literature.[10] The cross section is factored into two parts, the t-matrix part determining the momentum transfer and the form-factor part determining the probability amplitude for the given momentum transferred. For homonuclear diatomic molecules, the contributions from the two target atoms are equal in magnitude, and the phase factors are such that only $\Delta j=$even transitions are allowed. The total cross section is obtained from the differential cross section by the relation

$$\sigma(vjp_3\rightarrow v'j'p_3')=\frac{2\pi}{p_3p_3'}\int_{|p_3-p_3'|}^{p_3+p_3'}\left|\frac{d\sigma}{d\Omega}\right|qdq\ . \tag{37}$$

IV. BEYOND THE PEAKING APPROXIMATION

It is useful to recall that the two-body t matrix depends upon the momenta q_s and q_s' and the angle between these momenta.[10,14,21] In terms of other momenta, this means that the matrix element depends upon incident momentum $\mathbf{p}_3$, internal molecular momentum $\mathbf{q}_3$, and momentum transferred during the collision, $\mathbf{q}$. Of these, only $\mathbf{p}_3$ and $\mathbf{q}$ are observables. To proceed beyond the peaking approximation, the variation of the two-body t matrix must be properly taken into account over the range of integration in $\mathbf{q}_3$ in Eq. (22). This is nontrivial, but can be accomplished as follows. We first note that the final-state wave function in the momentum representation is obtained from the final-state wave function in the coordinate representation by the Fourier transform,

$$\phi^{*'}(\mathbf{q}_3')=(2\pi)^{-3/2}\int d\mathbf{r}\exp(-i\mathbf{q}_3\cdot\mathbf{r})\times\exp(-i\alpha_s\mathbf{q}\cdot\mathbf{r})\psi^{*'}(\mathbf{r})\ , \tag{38}$$

where we have written $\mathbf{q}_3'=\mathbf{q}_3+\alpha_s\mathbf{q}$, and α_s has been defined earlier [Eq. (31)]. We now define a function $\psi^{(s)}(\mathbf{r})$ by the relation

$$\psi^{(s)}(\mathbf{r})\equiv(2\pi)^{-3/2}\int d\mathbf{q}_3\exp(-i\mathbf{q}_3\cdot\mathbf{r})\langle\mathbf{q}_s'|t^{(s)}|\mathbf{q}_s\rangle\phi(\mathbf{q}_3) \tag{39}$$

to obtain

$$\langle\phi_3'|T^{(s)}|\phi_3\rangle=\int d\mathbf{r}\,\psi^{*'}(\mathbf{r})\exp(-i\alpha_s\mathbf{q}\cdot\mathbf{r})\psi^{(s)}(\mathbf{r})\ . \tag{40}$$

Now we expand the two-body t matrix in a spherical harmonics expansion in the angle $\hat{q}_3$ as

$$\langle\mathbf{q}_s'|t^{(s)}|\mathbf{q}_s\rangle=\sum_{L,M}t_{LM}^{(s)}(q_3,\mathbf{p}_3,\mathbf{q})Y_{LM}(\hat{q}_3)\ , \tag{41}$$

with $t_{LM}^{(s)}$ given by

$$t_{LM}^{(s)}(q_3,\mathbf{p}_3,\mathbf{q})=\int d\hat{q}_3\,Y_{LM}^{*}(\hat{q}_3)\langle\mathbf{q}_s'|t^{(s)}|\mathbf{q}_s\rangle\ . \tag{42}$$

Substituting this expansion into Eq. (39), and introducing the plane-wave expansion,

$$\exp(-i\mathbf{q}_3\cdot\mathbf{r})=4\pi\sum_{\lambda,\mu}i^{(l-\lambda)}Y_{\lambda\mu}(\hat{r})Y_{\lambda\mu}^{*}(\hat{q}_3)j_{\lambda}(q_3r)\ , \tag{43}$$

we get

$$\psi^{(s)}(\mathbf{r})=\sum_{L,M,\lambda,\mu}i^{(j-\lambda)}K_{LM\lambda}^{(s)}(r)Y_{\lambda\mu}(\hat{r})\left|\frac{\hat{j}\hat{L}}{4\pi\hat{\lambda}}\right|^{1/2}\times C(jL\lambda;00)C(jL\lambda;mM)\ , \tag{44}$$

where

$$K_{LM\lambda}^{(s)}(r)=\frac{2}{\pi}\int_0^{\infty}dq_3q_3^2j_{\lambda}(q_3r)t_{LM}^{(s)}(q_3,\mathbf{p}_3,\mathbf{q})I_{vj}(q_3) \tag{45}$$

and $I_{vj}(q_3)$ is defined by Eq. (13).

Equation (40) has the form of an overlap integral, if $\psi^{(s)}$ is viewed as the *effective* initial state that incorporates the modification to the original wave function produced by a nonconstant t matrix. In the peaking approximation, the $\mathbf{q}_3$ variation of $\langle \mathbf{q}_s' | t^{(s)} | \mathbf{q}_s \rangle$ is ignored, and Eq. (39) is approximated by evaluating this matrix element at some specific, fixed value of $\mathbf{q}_3$, leading immediately to the simplified form

$$\psi^{(s)}(\mathbf{r}) = t_{\mathrm{PA}}^{(s)} \psi(\mathbf{r}) , \tag{46}$$

and Eq. (40) then reduces to Eq. (28) of the preceding section. In terms of the spherical harmonics expansion for $t^{(s)}$, Eq. (41), it is as if $t^{(s)}$ is isotropic, i.e., only the $L=0$, $M=0$ term is nonzero, and also independent of the magnitude of q_3. Then,

$$\langle \mathbf{q}_s' | t^{(s)} | \mathbf{q}_s \rangle \to Y_{00} t_{00}^{(s)}(q_3) \to Y_{00} t_{00}^{(s)} \equiv t_{\mathrm{PA}}^{(s)} , \tag{47}$$

and Eqs. (44) and (45) lead to Eq. (46). The important point about the modification brought about by the variation of the matrix element of $t^{(s)}$ over $\mathbf{q}_3$ is that various terms now comprising the modified wave function interfere to produce the final scattering amplitude. So, even if the variation of $t^{(s)}$ over $\mathbf{q}_3$ is not significant and the nonisotropic modifying terms are small, their influence on the final result can be substantial. Ignoring this is the major problem with the PA.

To evaluate the integral in Eq. (40), we substitute another plane-wave expansion,

$$\exp(-i\alpha^{(s)}\mathbf{q}\cdot\mathbf{r}) = 4\pi \sum_{\beta,\gamma} (\pm i)^{\beta} Y_{\beta\gamma}(\hat{r}) Y_{\beta\gamma}^{*}(\hat{q}) j_{\beta}(|\alpha_s| qr) , \tag{48}$$

with the plus sign for $s=1$ and the minus sign for $s=2$. Then,

$$\langle \phi_3' | T^{(s)} | \phi_3 \rangle = \sum_{\beta,\lambda,\gamma,\mu,L,M} (\pm i)^{\beta} i^{(j-\lambda)} \left[\frac{\hat{j}\hat{L}\hat{\beta}}{\hat{j}'} \right]^{1/2} Y_{\beta\gamma}^{*}(\hat{q}) N_{LM\lambda\beta}^{(s)}(\mathbf{q},\mathbf{p}_3) C(jL\lambda;00) C(jL\lambda;mM\mu) C(\lambda\beta j';\mu\gamma m') , \tag{49}$$

where

$$N_{LM\lambda\beta}^{(s)}(\mathbf{q},\mathbf{p}_3) = \int dr\, r^2 j_{\beta}(|\alpha_s| rq) K_{LM\lambda}^{(s)}(r) \chi_{v'j'}(r) . \tag{50}$$

To simplify Eq. (49) for computational purposes, it is convenient to choose the z axis of the coordinate system along $\mathbf{q}$, the direction of momentum transfer vector. Then,

$$Y_{\beta\gamma}^{*}(\hat{q}) = \left[\frac{\hat{\beta}}{4\pi} \right]^{1/2} \delta_{\gamma 0} . \tag{51}$$

Using the properties of Clebsch-Gordan coefficients, we note that, in Eq. (49), only the $\mu = m'$ term is nonzero and $M \equiv (m'-m)$. Noting the identity[20]

$$C(jL\lambda;m,M) C(\lambda\beta j';m+M,0) = \sum_{J} W(jLj'\beta;\lambda J) (\hat{\lambda}\hat{J})^{1/2} \times C(jJj';m,M) C(L\beta J;M,0) , \tag{52}$$

we get a relation between the total angular-momentum change during the collision, J, and the initial and final rotational quantum numbers j and j'. We also note the total angular-momentum change J is composed of two parts: L, coming from the two-body t matrix, and β, the usual component, derived from the momentum transferred during the collision. Substituting Eq. (52) into Eq. (49), we get

$$\langle \phi_3' | T^{(s)} | \phi_3 \rangle = \sum_{\beta,\lambda,L,J} (\pm i)^{\beta} i^{(j-\lambda)} \left[\frac{\hat{j}\hat{L}\hat{\lambda}\hat{J}}{4\pi \hat{j}'} \right]^{1/2} \hat{\beta} N_{LM\lambda\beta}^{(s)}(q) C(jL\lambda;00) \times C(\lambda\beta j';00) C(jJj';mM) C(L\beta J;M0) W(jLj'\beta;\lambda J) . \tag{53}$$

The expression for the differential cross section is now obtained by summing the absolute square of the collision amplitude over m and m'. Since $M = m'-m$, one can instead sum over m and then over M. Summation over m, for fixed M, leads to

$$\sum_{m} C(jJj';mM) C(j\bar{J}j';mM) = \left[\frac{\hat{j}'}{\hat{J}} \right] \delta_{J\bar{J}} , \tag{54}$$

where the second factor on the left-hand side comes from the complex conjugate of Eq. (53). Carrying out the m and the $\bar{J}$ sums, we finally obtain

$$\frac{d\sigma}{d\Omega}(vjp_3 \to v'j'p_3', \theta) = \left[\frac{2\pi}{\hbar} \right]^4 \mu_3^2 \frac{p_3'}{p_3} \sum_{J=|j-j'|}^{J=(j+j')} \sum_{M} |F_{JM}|^2 , \tag{55}$$

where

$$F_{JM}=\sum_{L,\beta,\lambda}(i)^{(j-\lambda+\beta)}\hat{\beta}\left[\frac{\hat{L}\hat{\lambda}}{4\pi}\right]^{1/2}C(jL\lambda;00)C(\lambda\beta j';00)C(L\beta J;M0)W(jLj'\beta;\lambda J)[N^{(1)}_{LM\lambda\beta}+(-1)^{\beta}N^{(2)}_{LM\lambda\beta}]\ . \tag{56}$$

This is the central result of this paper, invoking no approximations in evaluating the differential cross section in the impulse approach, Eq. (23). The integrations and summations become possible by separating angular parts of all relevant expressions and repeated use of angular-momentum identities. It should be noted that no assumptions were necessary regarding the structure or the properties of the t matrix. We have only invoked the completeness of the spherical harmonics expansion, Eq. (41), in arriving at this result. Equation (55) then constitutes the full calculation of the differential cross section in the impulse approach for any two-body potential.

To see how Eqs. (55) and (56) reduce to the PA, we note that, in the PA, $t^{(s)}$ is assigned some fixed value independent of $\mathbf{q}_3$, i.e.,

$$t(\mathbf{q}_3,\mathbf{p}_3,\mathbf{q})\rightarrow t^{(s)}(\mathbf{p}_3,\mathbf{q})_{\mathrm{PA}}\ .$$

Thus $L=M=0$ is the only nonzero term in Eqs. (41) and (42), and

$$t^{(s)}_{00}=\sqrt{4\pi}\,t^{(s)}_{\mathrm{PA}}\ ; \tag{57}$$

all other $t^{(s)}_{LM}=0$, and we can set $L=0$ and $M=0$ in Eq. (56). Then,

$$C(0\beta J;00)=\delta_{\beta J}\ , \tag{58}$$

$$C(j0\lambda;00)=\delta_{j,\lambda}\ , \tag{59}$$

$$W(j0j'J;jJ)=(\hat{j}\hat{J})^{-1/2}\ , \tag{60}$$

and

$$N^{(s)}_{00jJ}=\sqrt{4\pi}f^{(s)}_{v'j',vj;J}t^{(s)}_{\mathrm{PA}}\ ; \tag{61}$$

all other $N_{LMjJ}=0$.

When Eqs. (57)–(61) are substituted in Eq. (55), we get

$$\frac{d\sigma}{d\Omega}(vjp_3\rightarrow v'j'p'_3,\theta)=\left[\frac{2\pi}{\hbar}\right]^4\mu_3^2\frac{p'_3}{p_3}\sum_{\beta=j'-j}^{j'+j}C^2(j\beta j';00)\hat{\beta}|f^{(1)}_{v'j',vj;\beta}t^{(1)}_{\mathrm{PA}}+(-1)^{\beta}f^{(2)}_{v'j',vj;\beta}t^{(2)}_{\mathrm{PA}}|^2\ . \tag{62}$$

Noting that β has the same parity as Δj, we recover the PA formula, Eq. (36). We have written $\equiv$ instead of $=$ in Eq. (61) to emphasize that $N^{(s)}$ is based on the averaged isotropic component of $t^{(s)}$, whereas the PA evaluates $t^{(s)}$ at a given fixed value of the spectator momentum, and thus ignores the dependence on the molecular momentum $\mathbf{q}_3$. One can take advantage of the simplification afforded by the angular-momentum algebra without completely sacrificing the q_3 dependence of $t^{(s)}$ by taking just the isotropic component of the t matrix, leading to

$$N^{(s)}_{00jJ}\neq 0\ , \tag{63}$$

all other $N^{(s)}_{LMjJ}=0$. We again recover the PA formalism, with $N^{(s)}_{00jJ}$ replacing $\sqrt{4\pi}f^{(s)}t^{(s)}_{\mathrm{PA}}$ in Eq. (62). We might call this the isotropic approximation. Although the algebra involved becomes the same, the numerical results may be quite different.

V. COMPARISON OF THE EXACT AND PA RESULTS

In this section, we compare the results obtained by our exact calculation [Eq. (55)] with those obtained by using the PA [Eq. (36)]. We use both formulations to compute the differential and total cross sections for the much-studied process[8,14,15]

$$\mathrm{Li}^+ + \mathrm{N}_2(v,j)\rightarrow \mathrm{Li}^+ + \mathrm{N}_2(v',j')\ . \tag{64}$$

For homonuclear diatoms, the two amplitudes corresponding to $s=1,2$ are equal in magnitude. The relative phase of these amplitudes can be established by noting

$$\langle \mathbf{q}'_1|t(1)|\mathbf{q}_1\rangle(\mathbf{q}_3)=\langle \mathbf{q}'_1|t(2)|\mathbf{q}_1\rangle(-\mathbf{q}_3) \tag{65}$$

giving

$$t^{(1)}_{LM}=(-1)^L t^{(2)}_{LM} \tag{66}$$

and

$$N^{(1)}_{LM\lambda\beta}=(-1)^L N^{(2)}_{LM\lambda\beta}\ . \tag{67}$$

Since $L+\beta$ must have the same parity as Δj for the Clebsch-Gordan coefficients in Eq. (56) to be nonzero, the last factor in that equation simplifies to

$$[N^{(1)}_{LM\lambda\beta}+(-1)^{\beta}N^{(2)}_{LM\lambda\beta}]\rightarrow[1+(-1)^{\Delta j}]N^{(1)}_{LM\lambda\beta}\ . \tag{68}$$

Thus, $\Delta j=$odd transitions vanish, and the calculations for the $\Delta j=$even processes are simplified.

The two-body interaction is represented by a hard-core potential, for which the t matrix is available in a closed form.[21] Since this is the only potential used in the previous studies, a direct comparison of our results with those of previous studies is possible. The two-body t-matrix element is

$$\langle \mathbf{q}'_i|t^{(s)}(\epsilon_i)|\mathbf{q}_i\rangle\equiv t^{(s)}(\mathbf{q}'_i,\mathbf{q}_i,\epsilon_i)\ , \tag{69}$$

where $\epsilon_i=q_i^2/2\mu_{iu}$ is the relative translational energy of

the two colliding atoms, t and u, and is related to the three-body kinetic energy E_0 by the relation

$$E_0 \equiv p_3^2/2\mu_3 + q_3^2/2\mu_{12} = p_s^2/2\mu_s + q_s^2/2\mu_{tu} . \quad (70)$$

The matrix elements in Eq. (69) are called half-on-energy shells since the energy of the final state $\langle \mathbf{q}_s' |$ is not equal to that of the initial state $|\mathbf{q}_s\rangle$, which has the physical energy. This choice of the t matrix is called the "post" form.[10] The other choice of the t matrix $t^{(s)}(\mathbf{q}_s', \mathbf{q}_s, \varepsilon_s')$ is called the "prior" form. Since $\varepsilon_s' \equiv q_s'^2/2\mu_{tu} \neq \varepsilon_s$, the two sets of matrix elements can differ substantially under some circumstances. This difference has been termed the "post-prior discrepancy."

The needed vibration-rotation wave functions for N_2 were obtained by numerical integration of the Schrödinger equation. The intramolecular potential function used for N_2 was constructed from spectroscopic constants[22] using the Rydberg-Klein-Rees method.[23]

The computations are carried out as follows. The matrix element $t^{(1)}(\mathbf{q}_1', \mathbf{q}_1, \varepsilon_1)$ is evaluated using Eqs. (33) and (39) of Eckelt *et al.*,[10] and the partial waves t_l are summed until the desired convergence is attained. We use the exact expression for the angle between $\mathbf{q}_1$ and $\mathbf{q}_1' \equiv \mathbf{q}_1 + \mathbf{q}$. The range of interest for $\mathbf{q}_1$ is given by

$$\mathbf{q}_1 = \{1 - [m_1/(m_1+m_2)][m_3/(m_2+m_3)]\}\mathbf{p}_3 - [m_3/(m_2+m_3)]\mathbf{q}_3 , \quad (71)$$

obtained by eliminating $\mathbf{p}_1$ from Eqs. (16) and (18). It is convenient to choose the coordinate axis so that $\mathbf{q}$, the momentum transferred, is along the z axis; $\mathbf{p}_3$ is taken in the z-x plane. $\mathbf{p}_3' \equiv \mathbf{p}_3 + \mathbf{q}$, then, is also in the z-x plane at the center-of-mass scattering angle θ. The range of $\mathbf{q}_3$ is determined by the wave function of the initial state in the momentum space, $\phi(\mathbf{q}3)$. The coefficients $t_{LM}(q_3, \mathbf{p}_3, q)$ are determined by integrating the product of $t^{(1)}(\mathbf{q}_1', \mathbf{q}_1, \varepsilon_1)$ and $Y_{LM}^*(\hat{q}_3)$ over the direction of $\mathbf{q}_3$, Eq. (42). Subsequent integration over the magnitude q_3 leads to $K_{LM\lambda}^{(1)}$, the radial component of the wave function of the effective initial state $\psi^{(1)}$, i.e., the initial-state wave function modified by the t matrix, Eqs. (44) and (45). Integration of $K_{LM\lambda}^{(1)}$ over r, weighted by the amplitude of the momentum transferred, q, and the final-state wave function, Eq. (50), gives $N_{LM\lambda\beta}^{(1)}$, the dynamical component of the transition matrix between initial and final states, Eq. (53).

The typical number of points required to obtain a significant sixth figure is as follows: 64 points for the integration over the direction of $\hat{q}_3$ (eight points for the polar angle and eight points for the azimuthal angle), 120 points for the magnitude of q_3, and 70 points for the integration over r.

Now we study the excitation of N_2 from the ground state ($v=0$ and $j=0$) during collision with Li^+. The exact and PA results for this process, Eq. (64), at a relative translational energy of 1 eV, are shown by plotting the differential cross section, at a c.m. scattering angle of 30°, as a function of energy loss $\Delta\varepsilon = E_{rel} - E_{rel}' = (p_3^2 - p_3'^2)/2\mu_3$, for $v'=0$ and 1 in Fig. 1 and $v'=2$ and 3 in Fig. 2. The same differential cross section, at a c.m. scattering angle of 150°, is plotted as a function of energy loss for $v'=0$ and 2 in Fig. 3, and for $v'=1$ and 3 in Fig. 4. The hard-core radius for the Li^+-N two-body collision is taken to be 1.62 Å for this energy.[10] For deexcitation processes ($\Delta\varepsilon < 0$), we find, in Fig. 5, that the PA, except for small angles (where the IA is of dubious validity[19]), underestimates the exact IA results. Thus, we conclude that the PA overestimates (underestimates) the exact IA cross section for the excitation (deexcitation) process. It is interesting to note that both the PA and exact calculations lead to the same general pattern for the differential cross section. The oscillatory structure of the state-to-state differential cross sections, especially the sharp final peak calculated for each v' termed "rotational rainbow structure,"[8] is exhibited both by the PA and the exact calculation. This similarity of patterns is a reflection of

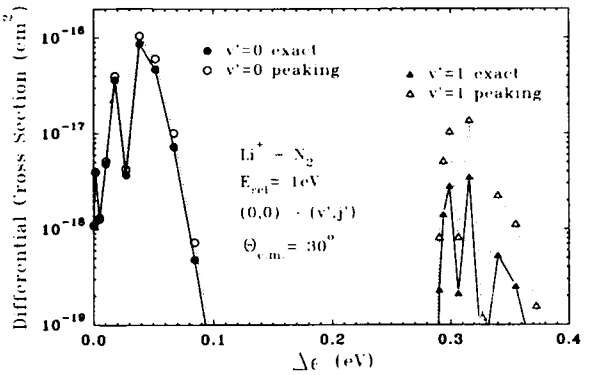

FIG. 1. Differential cross section (cm^2) for the exact and PA calculations vs energy loss (eV) for the c.m. scattering angle of 30° and for the collision process $Li^+ + N_2(v=0, j=0) \rightarrow Li^+ + N_2(v', j')$, at an initial relative translational energy of 1 eV. The peaking calculation (○ for $v'=0$ and △ for $v'=1$) gives a larger cross section than the exact calculation (solid symbols).

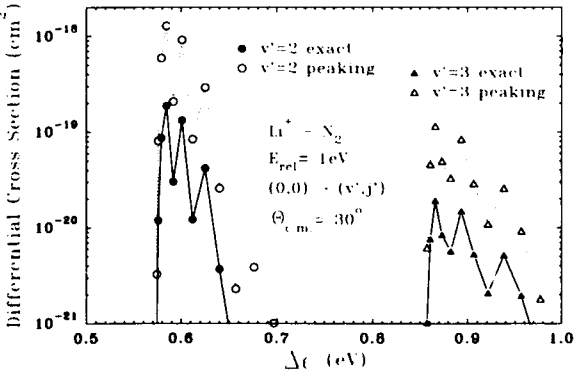

FIG. 2. Differential cross section (cm^2) for the exact and PA calculations vs energy loss (eV) for the c.m. scattering angle of 30° and for the collision process $Li^+ + N_2(v=0, j=0) \rightarrow Li^+ + N_2(v', j')$, at an initial relative translational energy of 1 eV. The peaking calculation (○ for $v'=2$ and △ for $v'=3$) gives a larger cross section than the exact calculation (solid symbols).

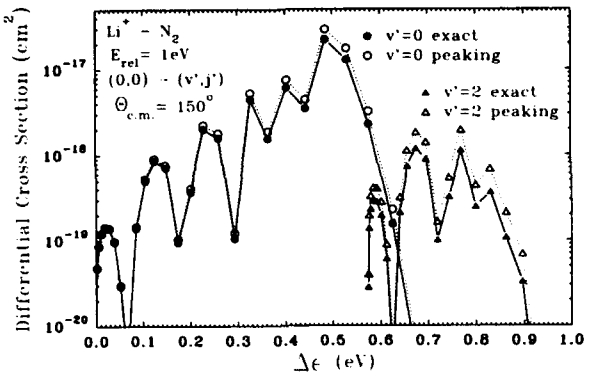

FIG. 3. Differential cross section (cm^2) for the exact and PA calculations vs energy loss (eV) for the c.m. scattering angle of 150° and for the collision process $Li^+ + N_2(v=0, j=0) \rightarrow Li^+ + N_2(v', j')$, at an initial relative translational energy of 1 eV. The peaking calculation (○ for $v'=0$ and △ for $v'=2$) gives a larger cross section than the exact calculation (solid symbols). Notice the larger rotational excitation than that for 30° scattering.

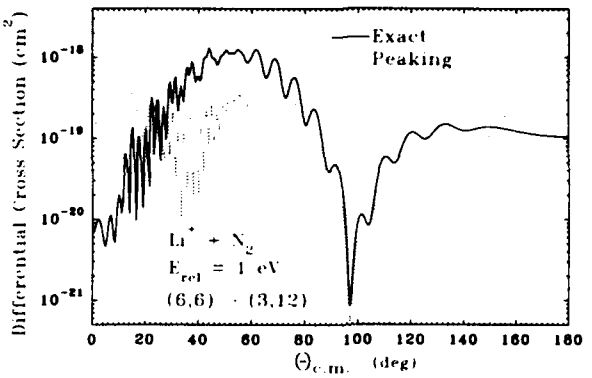

FIG. 5. Differential cross section (cm^2) for the exact and PA calculations as a function of the center-of-mass scattering angle (deg) for the deexcitation process $Li^+ + N_2(6,6) \rightarrow Li^+ + N_2(3,12)$ at a relative translational energy of 1 eV.

the fact that small $L \neq 0, M = 0$ terms in Eq. (56) interfere with the dominant isotropic term. It has been pointed out earlier[15] that keeping only the isotropic ($L = 0$) term has the same mathematical structure as the PA but with a different t matrix. This interference between different L terms modifies the numerical value of the differential cross section, keeping the general pattern intact. This point is further discussed in Sec. VII.

Finally, we display the total cross section $\sigma_T(00 \Rightarrow v'j')$ for the $Li^+ + N_2$ collisions at relative translational energies of 1 eV (Fig. 6) and 10 eV (Fig. 7). It should be noticed that for vibrationally inelastic collisions the cross section increases rapidly at the threshold, stays constant as higher rotational levels are populated with greater energy loss, and then falls rapidly. For 1-eV relative translational energy and final vibrational levels $N_2(v'=2$ and 3), this fall occurs when the available energy is almost totally depleted. This result is consistent with the measurements of Loesch and Herschbach[24] who, in their work on crossed beams of Ar and CsI at collision energies of 0.35–1.1 eV, found peaks that "correspond to an extremely inelastic 'ballistic' process in which most of the initial relative translational energy goes into vibrational or rotational excitation." King, Loesch, and Herschbach reported[25] similar observations from a crossed-beam study of Ar and CsF at a relative kinetic energy of 0.66 eV. For $N_2(v'=0)$, the excitation cross section drops off dramatically when about half of the available translational energy goes into rotational energy. This is because when momentum q is transferred to the molecule, its rotational quantum number may be altered by up to $|\alpha_s| bq$, where b is the internuclear distance of the diatom, to conserve total angular momentum. Further, if the molecule is initially moving slowly or is at rest in the

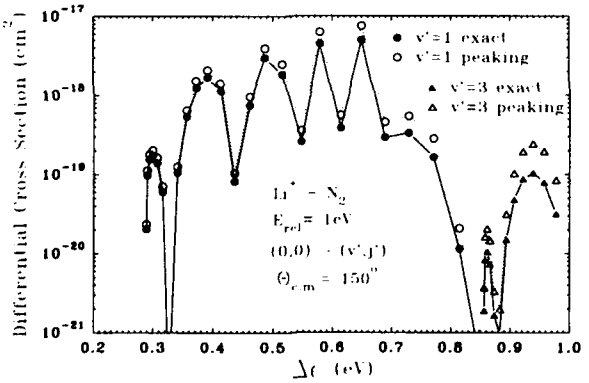

FIG. 4. Differential cross section (cm^2) for the exact and PA calculations vs energy loss (eV) for the c.m. scattering angle of 150° and for the collision process $Li^+ + N_2(v=0, j=0) \rightarrow Li^+ + N_2(v', j')$, at an initial relative translational energy of 1 eV. The peaking calculation (○ for $v'=1$ and Δ for $v'=3$) gives a larger cross section than the exact calculation (solid symbols). Again, notice the larger rotational excitation than that for 30° scattering.

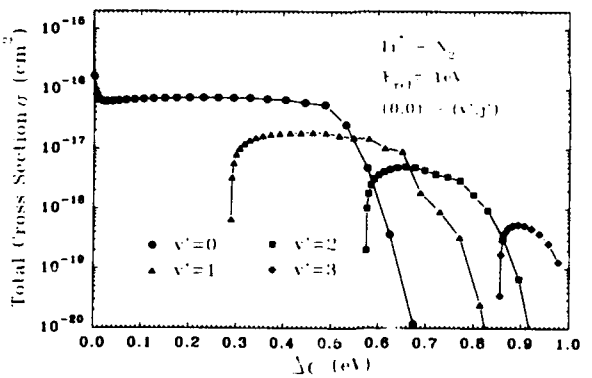

FIG. 6. Total cross section according to the exact calculation as a function of energy loss for the collision of N_2 with Li^+, at a relative translational energy of 1 eV. The molecule is initially in the $v=0$ and $j=0$ states. Final vibrational states are denoted as follows: ○, $v'=0$; △, $v'=1$; □, $v'=2$; and ◇, $v'=3$. Final rotational states, j', increase sequentially from left to right, starting with $j'=0$ in steps of 2. Notice that almost all the translational energy may be converted into internal degrees of freedom.

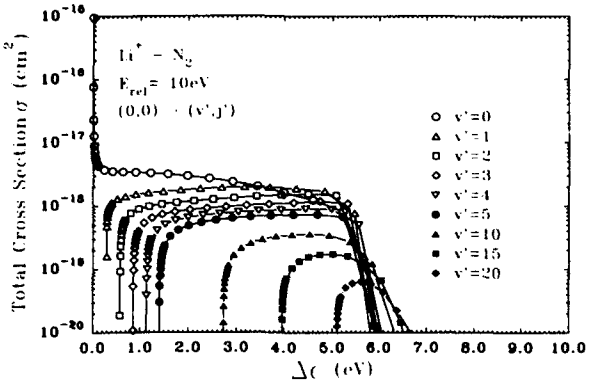

FIG. 7. Same as Fig. 5, but with $E_{rel}=10$ eV. Several final vibrational states are shown, with symbols as defined in the figure. A precipitous drop in the excitation cross sections is to be noticed.

laboratory frame, it acquires $[1/2(m_1+m_2)]q^2$ kinetic energy to conserve the total linear momentum. The physical picture that emerges is that if the momentum transferred is comparable to the momentum of the center of mass of the molecule, we observe the "ballistic" phenomenon. On the other hand, when the momentum transferred is much larger than the c.m. momentum and the molecule is excited to very high rotational or vibrational levels, not all the initial relative translational energy can be converted into internal energy. This feature was evident in the experiment of Hershberger *et al.*,[26] who observed that during the collisions of CO_2 gas at room temperature with energetic H, D, and Cl atoms, the molecules excited to higher rotational levels are also the ones moving at greater speeds.

VI. INTERNAL CONSISTENCY OF THE CALCULATED CROSS SECTIONS

The previous sections have shown how to do an exact calculation of the inelastic atom-diatom cross sections using the IA formalism. In this section, we check the results for internal consistency by testing them for semidetailed balancing (SDB).

The Hamiltonian is independent of time and quadratic in momenta, and is, therefore, invariant under time reversal (TR). This symmetry, together with space invariance, requires[27] that the exact scattering amplitudes obey the SDB relation between the differential cross sections for the forward and reverse processes, i.e.,

$$p[d\sigma(i\to f)/d\Omega]/\rho(f)=p'[d\sigma(f\to i)/d\Omega]/\rho(i)\ , \tag{72}$$

where $\rho(i)$ and $\rho(f)$ are the densities of state in the initial and final states; p and p' represent the incident flux densities for the direct and reverse processes. It was shown earlier[18] that the differential cross sections for the rotational-vibrational excitation of N_2 upon collision with Li^+ do not satisfy SDB for small scattering angles. The scattering amplitudes for the forward process using the post model of the two-body energy parameter and the reverse process using the prior model of the two-body energy parameter are the same (Appendix A), apart from an overall sign factor and change in the sign of the magnetic quantum numbers ($m\to -m$ and $m'\to -m'$). We have, therefore, the general result that the differential cross sections for the forward and the reverse process are related by the density-of-states factors. Thus, the failure of the post model to satisfy SDB also implies the corresponding failure of the prior model. That these two models are not adequate for describing the collision process for all angles is shown by the fact that the total scattering cross section using these models for two-body energy is much less than the geometric shadow. The "full" model[14] of the two-body energy parameter z_{1A} obeys SDB for all angles, but, as has been noted earlier,[18] suffers from other difficulties, one being that the total calculated cross section is far in excess of the geometric shadow.

For large scattering angles, the differential cross section was shown[18] to be rather insensitive to the model used for the two-body energy parameter z_{1A}. This can be understood as follows. The two-body scattering amplitude from a hard-core potential for large scattering angles, provided $q_s r_c \gg 1$, is constant, independent of collision energy, as long as the ratio of the incident to the final momentum stays the same (Fig. 8) (the two-body scattering angle is denoted by ϕ while the three-body scattering angle is represented by θ). On the energy shell, i.e., $q_s^2=q_s'^2$, this value[28] is $r_c/2$. The equivalent classical process would be the energy-conserving on-the-energy-shell process, one with ratio $q_s/q_s'=1$. Using the relation $\mathbf{q}_s'=-(-1)^s\mathbf{q}+\mathbf{q}_s$, and recalling that the z axis in this calculation is taken along the momentum transfer vector $\mathbf{q}$, the on-the-energy-shell requirement becomes $-(-1)^s 2q_{sz}q+q^2=0$, q_{sz} being the z component of $\mathbf{q}_s$. The root $q=0$ corresponds to forward scattering with no change of momentum, and in the classical picture it corresponds to no collision. The root $q_{sz}=(-1)^s q$, leading to $q_{sz}'=q_{sz}$, corresponds to the situation in which the z component of the incident momentum changes sign, and

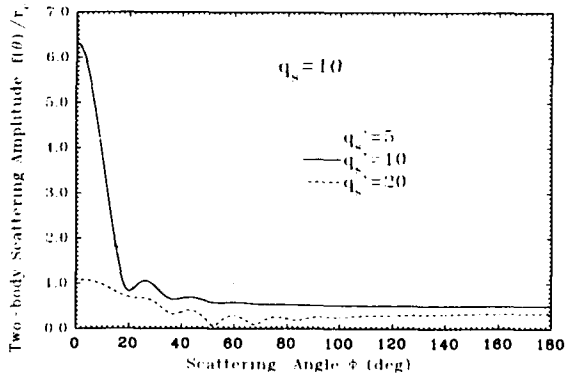

FIG. 8. Absolute value of the two-body scattering amplitude divided by the range of the hard-core potential, as a function of the two-body scattering angle ϕ, for an incident momentum of 10^9 cm^{-1}. An asymptote of 0.5 is reached for the on-the-energy-shell process.

the x and y components remain unaffected. This is very much the description of a collision between two hard spheres using classical mechanics.[29] We still compute the two-body t matrix quantum mechanically, so we call the on-the-energy-shell ($q_i^2 = q_i'^2$) two-body t matrix the semiclassical t matrix. Using the relation $p_{3z} = -\mu_3(\Delta\varepsilon/q) + (q/2)$, where $\Delta\varepsilon$ is the energy gained by the internal degrees of freedom of the molecule, and Eqs. (16)–(19), we can write

$$q_{3z}^{SC} = -(\alpha_i q/2) + (\mu_{12}\Delta\varepsilon/\alpha_i q) . \tag{73}$$

Recalling that q_3 is the relative momentum of the two atoms in the diatom, we note that Eq. (73) restricts the value of the component of $\mathbf{q}_3$ along the momentum transfer vector $\mathbf{q}$, in order for the molecule to gain energy $\Delta\varepsilon$ by the energy-momentum conservation relations for scattering between two hard spheres.

Relation (73) also results from quantum mechanics if q_{3z}^{SC} is defined as the weighted average

$$q_{3z}^{SC} \equiv \frac{\int \phi^* q_{3z} \phi d\mathbf{q}_3}{\int \phi^* \phi d\mathbf{q}_3} . \tag{74}$$

Relation (74) is proved in Appendix B. Because the derivation of Eq. (74) does not use the properties of scattering from a hard sphere, Eq. (73) is a more general relation. We can then conclude that large-angle scattering can be described by on-the-energy-shell matrix elements using the two-body t matrix for any potential. To demonstrate the accuracy of these conclusions, we plot in Fig. 9 the differential cross section versus the angle for the exact calculation and the semiclassical calculation using the on-the-energy-shell two-body t matrix evaluated at fixed $q_{3z} = q_{3z}^{SC}$, given by Eq. (73). The transverse momenta q_{3x} and q_{3y} still range over the entire x-y plane. The two calculations agree well at large angles, showing that for these angles the two-body scattering is effectively, indeed, an on-the-energy-shell process. A semiclassical calculation restricting $q_{3x} = q_{3y} = 0$ in the two-body t matrix is also shown in Fig. 9. The results are

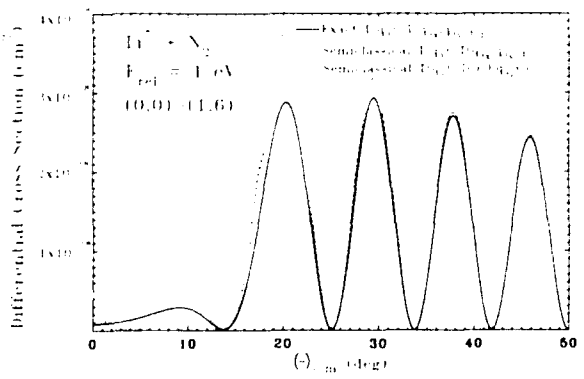

FIG. 9. Exact and two semiclassical differential cross sections as a function of the center-of-mass scattering angle, for $Li^+ + N_2(0,0) \rightarrow Li^+ + N_2(1,6)$. The two semiclassical calculations become identical for angles larger than about 16°. They also equal the exact calculation after about 35°.

exactly the same as from the calculation in which q_{3x} and q_{3y} are not restricted, if the c.m. scattering angle is $\geq 15°$. This simplification leads to an expression for the differential cross section identical to that given by the PA, except that the two-body t matrix is evaluated for q_{3z}^{SC} given by Eq. (73), instead of $q_{3z} = -\alpha_i q/2$. It is seen that in the region of validity of the IA, the two-body t matrix may be computed by the on-the-energy-shell semiclassical procedure. Further, the results obtained, at least for the hard-core repulsive potential, are independent of the model chosen (post or prior) for the two-body energy parameter, z_{IA}.

VII. ANALYTICAL APPROXIMATIONS

We now develop some analytical approximations which lead to a relatively simple expression for the differential cross section, even for small scattering angles. This gives us further insight into the IA, and allows us to understand the similarities of the exact and the PA cross sections displayed in an earlier section. In addition, it also provides an effective procedure, valid over a wide range of parameters, for obtaining the IA cross sections with much less computational effort. The analytical approximation developed in this section has an advantage over the semiclassical approach of the last section, because it is valid over a larger range of scattering angles. This approximation will make it possible to calculate the higher terms of the multiple-collision expansion of the three-body T matrix, Eq. (5), of which the IA constitutes the single-collision terms.

Our starting point is the observation (Fig. 10) that the two-body t matrix for the post and prior models is a linear function of q_{3z}. The corresponding results for the full model, however, cannot be expressed in so simple a form. Recalling that the value of $\mathbf{q}_3$ perpendicular to $\mathbf{q}$ has no effect on the value of the t matrix, the z axis is taken along $\mathbf{q}$, and q_{3x} and q_{3y} are set equal to zero. The expression for the two-body t matrix, in the post and prior forms, becomes

$$t^{(v)}(\mathbf{q}_3) \equiv \langle \mathbf{q}_i' | t^{(v)} | \mathbf{q}_i \rangle = [t(0) + q_{3z}(\partial t/\partial q_{3z})_0] . \tag{75}$$

In mathematical language, the neglect of q_{3x} and q_{3y} is justified by noting that $(\partial t/\partial q_{3x})_0$ and $(\partial t/\partial q_{3y})_0$ are negligible compared to their z counterpart. Physically, this means that the results for a hard-core potential are insensitive to the angle between the plane containing $\mathbf{p}_3$, $\mathbf{p}_3'$, and $\mathbf{q}$, and that containing $\mathbf{q}_i$, $\mathbf{q}_i'$, and $\mathbf{q}$, so the two planes can be taken to be coincident. We can now rewrite Eq. (22) as

$$\int \phi^* t(\mathbf{q}_3) \phi d\mathbf{q}_3 \approx t(0) \int \phi^* \phi d\mathbf{q}_3 + (\partial t/\partial q_{3z})_0 \int \phi^* q_{3z} \phi d\mathbf{q}_3 . \tag{76}$$

The first integral in Eq. (76) is just the form factor of the molecule for the momentum transfer q,

$$F(q)=\int \phi^{*'}\phi d\mathbf{q}_3$$
$$=\int d\mathbf{r}\psi^{*'}(\mathbf{r})\exp(-i\alpha_3\mathbf{q}\cdot\mathbf{r})\psi(\mathbf{r})$$
$$=\langle f|e^{-i\alpha_3 zq}|i\rangle\ , \qquad (77)$$

where f and i denote the molecular final and initial states. This integral was evaluated earlier in Eqs. (28)–(35). The integral in the second term of Eq. (76) is shown in Appendix B to be q_{3z}^{SC} of Eq. (73) times form factor $F(q)$. The two-body t matrix now becomes

$$\int \phi^{*'} t(\mathbf{q}_3)\phi d\mathbf{q}_3 \approx \left| t(0)+q_{3z}^{SC}\left|\frac{\partial t}{\partial q_{3z}}\right|_0\right| F(q)\ . \qquad (78)$$

This is analogous to the peaking result, Eqs. (28) or (30), with t_{PA} replaced by the expression in the large square brackets. The remaining algebra for obtaining the differential cross section proceeds as in Eqs. (34)–(36). This explains why the shapes of the PA and exact differential cross sections are so similar.

A detailed comparison of the exact and analytical [Eq. (78)] calculations (using the post model) is presented in Fig. 11 for the collision of N_2 with Li^+. The analytical method of approximating the differential cross section has been found to agree with the exact calculation over a wide range of parameters when the two-body t matrix can be represented by the two-term expansion of Eq. (75). For the deexcitation processes, the analytical approximation also shows good agreement with the exact calculation, if the prior, rather than the post, model of the two-body t matrix is used. The post-prior discrepancy is likely to disappear for smaller angles as well upon the inclusion of the multiple-collision terms.

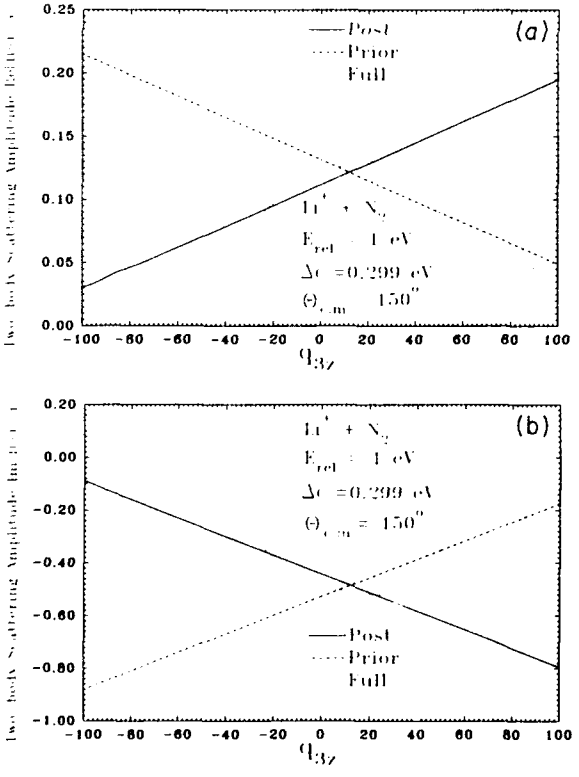

FIG. 10. (a) Real and (b) imaginary parts of the two-body scattering amplitude as a function of q_{3z}, the component of the internal momentum along the momentum transfer vector $\mathbf{q}$ for post, prior, and full models of the two-body energy parameter z_{1A}.

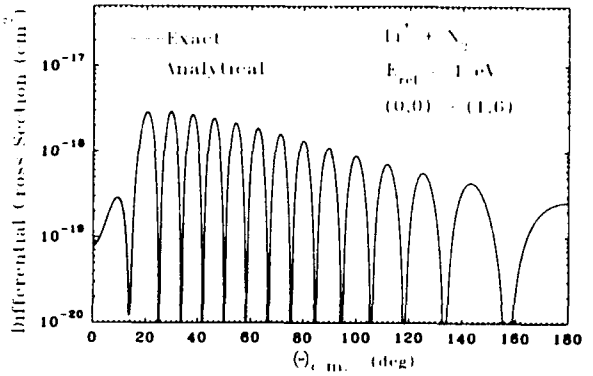

FIG. 11. Exact and analytical [based on Eq. (78)] differential cross sections, as a function of the c.m. scattering angle, for the collision of N_2 with Li^+ at a relative translational energy of 1 eV, for the transition (0,0 → 1,6).

VIII. COMPARISON OF THE COMPUTED AND EXPERIMENTAL RESULTS

We compare the results of our computations with the measurements of Böttner, Ross, and Toennies,[30] who crossed a Li^+ ion beam with a N_2 or CO beam. Figures 12 and 13 compare the total differential cross section as a function of the CM scattering angle at a relative transla-

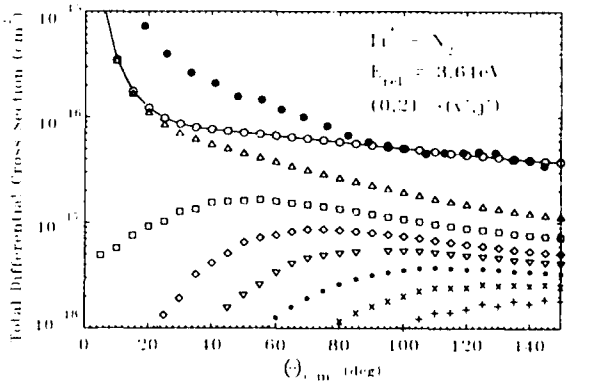

FIG. 12. Measured (solid circles) and calculated (open circles) total differential cross sections for the collision of $N_2(0,2)$ with Li^+, at a relative translational energy of 3.64 eV, as a function of the center-of-mass scattering angle. The experimental results, since they are not given in absolute units, are normalized to agree with the calculated ones at a scattering angle of 100°. We note that a substantial amount of energy goes into higher vibrational levels. Cross sections for the final vibrational levels, summed over the final rotational levels, are $v'=0(\triangle)$, $v'=1(\square)$, $v'=2(\diamond)$, $v'=3(\nabla)$, $v'=4(*)$, $v'=5(\times)$, and $v'=6(+)$.

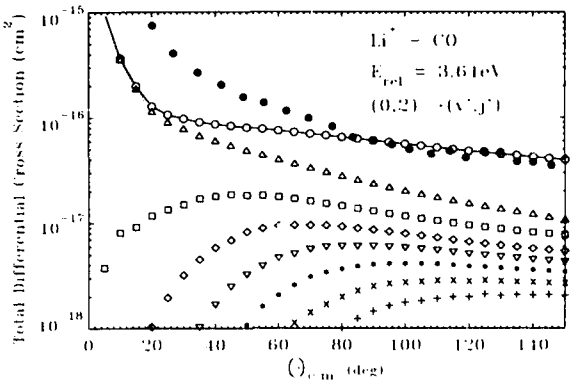

FIG. 13. Same as Fig. 12, except that the molecule is CO and the experimental points are now given in absolute units, the normalization being provided by the N_2 result of Fig. 12. The agreement of the calculation with the measurements is excellent.

tional energy of 3.64 eV for N_2 and CO, respectively. Measured cross sections are scaled to coincide with the calculated ones for N_2 at a scattering angle of 100°. As can be readily seen from the figures, the calculated and measured cross sections are in very good agreement for large angles. We give the contribution of various final vibrational levels to the total differential cross section. Finally, we plot (Fig. 14) differential cross sections for 49.2° at a relative translational energy of 4.23 eV as a function of the final rotational level (j') for the $v'=0$ and $v'=1$ levels of N_2. The calculated results have a very narrow distribution and are peaked at much higher rotational levels than the experimental data. Similar results were obtained for Li^+ and CO collisions. These results are largely a reflection of the hard-core two-body potential, which gives large and narrow momentum transfer $(-1)^{l}(q/2)=q_{sz}=-q'_{sz}$. A more realistic potential may give more reasonable results.

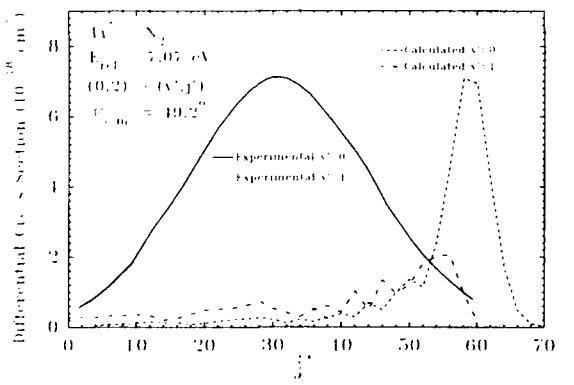

FIG. 14. Measured and calculated differential cross sections for the collision of $N_2(0,2)$ with Li^+, with a relative translational energy of 7.07 eV, at a center-of-mass scattering angle of 49.2° for final vibrational levels 0 and 1. The peak of the vibrationally elastic ($v'=0$) measured cross section is normalized to agree with the corresponding calculated cross section.

IX. CONCLUSIONS

A rather complete description of the exact formulation of the IA and its validity is given. On the formal side, the inclusion of the double and higher collision terms in the calculation, to be considered next, may render the formulation self-consistent for smaller scattering angles. It is pertinent to point out here that the IA is not an approximation to fully quantum coupled states or classical trajectory calculations. When the time duration of the collision is much smaller than the period of the characteristic motion of the diatom, the IA appears to be a more appropriate theory. In fact, classical trajectory calculations "so far have not been able to explain the observed distributions in rotational transition probabilities, consistently yielding distributions that are too narrow and peaked at smaller values ($j\approx 10$) than observed in the experiments ($j\approx 30$)".[31] This conclusion was also arrived at by Hershberger *et al.*[26] More realistic two-body potentials are currently being investigated in an attempt to use the IA to understand experiments involving large vibrational-rotational inelasticities.

The approach to vibration-rotation energy-transfer processes discussed here was first outlined by Landau and Teller,[32] who performed a one-dimensional calculation to obtain the vibration to translation rate coefficients. Subsequent authors, most notably Schwartz, Slawsky, and Herzfeld,[33] have expanded on the Landau-Teller work, however still keeping it a one-dimensional calculation. We have examined the basic ideas of these authors in the IA framework, elucidating the physics involved and formulating it in three dimensions to demonstrate the important role that the rotational degrees of freedom play in these processes. Our formulation treats the internal momentum of the diatom due to vibrational and rotational motion, $\mathbf{q}_3$, on an equal footing with the relative translational momentum, $\mathbf{p}_3$. This makes it possible for us to apply our calculation to collisions involving the intramolecular transfer of vibrational energy into rotational energy,[34] and the transfer of rotational energy into vibrational energy, as would be the case in a shock-tube experiment.[35] By doing an exact calculation on a simple potential, we have also been able to define the range of applicability of our calculation and the steps needed to extend this range.

APPENDIX A

The post model of the two-body t matrix upon time reversal (T_R) changes to the prior model and vice versa. This is seen by noting that incoming (outgoing) momenta become outgoing (incoming) momenta with a minus sign. Then,

$$T_R t_{\text{post}}(\mathbf{q}_s\rightarrow\mathbf{q}'_s)=T_R t\left|\mathbf{q}_s\rightarrow\mathbf{q}'_s;\varepsilon=\varepsilon_s=\frac{q_s^2}{2\mu_{tu}}\right.$$
$$=t\left|-\mathbf{q}'_s\rightarrow-\mathbf{q}_s;\varepsilon=\varepsilon_s=\frac{q_s^2}{2\mu_{tu}}\right.$$
$$=t_{\text{prior}}(-\mathbf{q}'_s\rightarrow-\mathbf{q}_s)\,. \qquad \text{(A1)}$$

Similarly,

$$T_R t_{\text{prior}}(\mathbf{q}_s \to \mathbf{q}_s') = t_{\text{post}}(-\mathbf{q}_s' \to -\mathbf{q}_s) . \tag{A2}$$

The wave functions are transformed under time reversal in the usual way.[27] Note, however, that the momentum transfer vector is invariant under T_R, $\mathbf{q} \equiv \mathbf{p}_3' - \mathbf{p}_3 = -\mathbf{p}_3 - (-\mathbf{p}_3')$. Invoking the property of the wave functions in momentum space,

$$\phi^*_{v,j,-m}(-\mathbf{q}_3) = (-1)^m \phi_{v,j,m}(\mathbf{q}_3) , \tag{A3}$$

it is straightforward to see, by a simple change of variables in Eq. (22), that the scattering amplitude for the forward process using the prior model of the two-body energy parameter is related to that of the reverse process using the post model,

$$A_{\text{prior}}(vjm, \mathbf{p} \to v'j'm', \mathbf{p}') = (-1)^{m'-m} A_{\text{post}}(v'j'-m', -\mathbf{p}' \to vj-m, -\mathbf{p}) . \tag{A4}$$

Using the space inversion invariance (which changes the sign of linear momenta), we have

$$A_{\text{post}}(v'j'-m', -\mathbf{p}' \to vj-m, -\mathbf{p}) = (-1)^{j'-j} A_{\text{post}}(v'j'-m', \mathbf{p}' \to vj-m, \mathbf{p}) . \tag{A5}$$

Combining Eqs. (A4) and (A5), we get

$$A_{\text{post}}(v'j'-m', \mathbf{p}' \to vj-m, \mathbf{p}) = (-1)^{j'+m'-j-m} A_{\text{prior}}(vjm, \mathbf{p} \to v'j'm', \mathbf{p}') . \tag{A6}$$

Taking the absolute square of both sides of Eq. (A6) and summing over m and m' leads to the desired relation between the forward and reverse processes.

APPENDIX B

We prove the relationship

$$q_{3z}^{\text{SC}} = \frac{\int \phi_f^* q_{3z} \phi_i d\mathbf{q}_3}{\int \phi_f^* \phi_i d\mathbf{q}_3} \tag{B1}$$

in this appendix. We start by rewriting the numerator in Eq. (B1) as

$$\int \phi^* q_{3z} \phi d\mathbf{q}_3 = \int d\mathbf{r} \psi^*(\mathbf{r}) \exp(-i\alpha_s \mathbf{q}\cdot\mathbf{r}) \hat{q}_{3z} \psi(\mathbf{r}) = \langle f | e^{-i\alpha_s z q} \hat{q}_{3z} | i \rangle . \tag{B2}$$

This is proved by using the defining relation for $\phi_i(\mathbf{q}_3)$, the molecular wave function in the momentum space in terms of $\psi_i(\mathbf{r})$, and the molecular wave function in the coordinate space,

$$q_{3z}\phi_i(\mathbf{q}_3) = (2\pi)^{-3/2} \int q_{3z} \exp[i(q_{3x}x + q_{3y}y + q_{3z}z)] \psi_i(\mathbf{r}) d\mathbf{r} = (2\pi)^{-3/2} \int dx\, dy \exp[i(q_{3x}x + q_{3y}y)] \int dz \left[-i\frac{\partial}{\partial z} \exp(iq_{3z}z) \right] \psi_i(\mathbf{r}) . \tag{B3}$$

Integrating by parts, we get

$$\int dz \left[-i\frac{\partial}{\partial z} \exp(iq_{3z}z) \right] \psi_i(\mathbf{r}) = -\int \exp(iq_{3z}z) \left[-i\frac{\partial}{\partial z} \psi_i(\mathbf{r}) \right] dz . \tag{B4}$$

Writing the defining relation for $\phi_f(\mathbf{q}_3')$, recalling that $\mathbf{q}_3' = \mathbf{q}_3 + \alpha_s \mathbf{q}$, and then integrating over $\mathbf{q}_3$ we get Eq. (B2), with

$$\hat{q}_{3z} = i\frac{\partial}{\partial z} .$$

Then, the exponential acts as a translation operator,

$$\exp(-i\alpha_s qz) f(\hat{q}_{3z}) \exp(i\alpha_s qz) = f(\hat{q}_{3z} - \alpha_s q) , \tag{B5}$$

because the momentum operator $\hat{q}_{3z}$ is conjugate to the coordinate operator z. Recalling that the Hamiltonian operator for the diatom is (setting $\hbar = 1$)

$$H = \frac{1}{2\mu_{12}} (\hat{q}_{3x}^2 + \hat{q}_{3y}^2 + \hat{q}_{3z}^2) + V(r_{12}) , \tag{B6}$$

where μ_{12} is the reduced mass and r_{12} is the internuclear distance of the diatom, we can rewrite Eq. (B5) as

$$[\exp(-i\alpha_s qz), H] = -\exp(-i\alpha_s qz) \frac{\alpha_s q}{2\mu_{12}} (\alpha_s q + 2\hat{q}_{3z}) , \tag{B7}$$

giving

$$\exp(-i\alpha_s qz)\hat{q}_{3z} = -\frac{\mu_{12}}{\alpha_s q} [\exp(-i\alpha_s qz), H] - \exp(-i\alpha_s qz)\frac{\alpha_s q}{2} . \tag{B8}$$

The matrix elements of the right-hand side of Eq. (B8) between the initial and final states give Eq. (B1).

[1]G. F. Chew, Phys. Rev. **80**, 196 (1950).
[2]G. F. Chew and G. C. Wick, Phys. Rev. **85**, 636 (1952).
[3]J. Ashkin and G. C. Wick, Phys. Rev. **85**, 686 (1952).
[4]G. F. Chew and M. L. Goldberger, Phys. Rev. **87**, 778 (1952).
[5]M. L. Goldberger and K. M. Watson, *Collision Theory* (Wiley, New York, 1964).
[6]L. S. Rodberg and R. M. Thaler, *Intoduction to the Quantum Theory of Scattering* (Academic, New York, 1967).
[7]J. P. Coleman, in *The Impulse Approximation and Related Methods in the Theory of Atomic Collisions*, Chap. 3 of *Case Studies in Atomic-Atomic Collisions*, edited by E. W. McDaniel and M. R. C. McDowell (North-Holland, Amsterdam, 1969).
[8]H. J. Korsch, H. Kutz, and H. D. Meyer, J. Phys. B **20**, 433 (1987); H. J. Korsch, H. D. Meyer, and C. P. Shukla, Z. Phys. D **15**, 227 (1990); A. Ernesti and H. J. Korsch, *ibid.* **16**, 201 (1990).
[9]A. Bogan, Jr., Phys. Rev. A **9**, 1230 (1974).
[10]P. Eckelt, H. J. Korsch, and V. Philipp, J. Phys. B **7**, 1649 (1974).
[11]H. J. Korsch and V. Philipp, Phys. Rev. A **13**, 497 (1976).
[12]V. Philipp, H. J. Korsch, and P. Eckelt, J. Phys. B **9**, 345 (1976).
[13]V. Philipp, H. J. Korsch, and P. Eckelt, J. Phys. B **10**, 117 (1977).
[14]L. H. Beard and D. A. Micha, J. Chem. Phys. **74**, 6700 (1981).
[15]R. D. Sharma, P. M. Bakshi, and J. M. Sindoni, Phys. Rev. A **40**, 1692 (1989).
[16]J. P. Coleman, J. Phys. B **1**, 567 (1968).
[17]R. D. Sharma, unpublished.
[18]R. D. Sharma, P. M. Bakshi, and J. M. Sindoni, Phys. Rev. A **41**, 6540 (1990).
[19]H. J. Korsch and R. Möhlenkamp, J. Phys. B **15**, 2187 (1982).
[20]M. E. Rose, *Elementary Theory of Angular Momentum* (Wiley, New York, 1957).
[21]J. M. J. Van Leeuwen and A. S. Reiner, Physica **27**, 99 (1961).
[22]K. P. Huber and G. Herzberg, *Constants of Diatomic Molecules* (Van Nostrand Reinhold, New York, 1979).
[23]J. I. Steinfeld, *An Introduction to Modern Molecular Spectroscopy* (MIT Press, Cambridge, 1985).
[24]H. J. Loesch and D. R. Herschbach, J. Chem. Phys. **57**, 2038 (1972).
[25]D. L. King, H. J. Loesch, and D. R. Herschbach, Discuss. Faraday Soc. **55**, 222 (1973).
[26]J. F. Hershberger, S. A. Hewitt, S. K. Sarkar, G. W. Flynn, and R. E. Weston, Jr., J. Chem. Phys. **91**, 4636 (1989).
[27]A. G. Sitenko, *Lectures in Scattering Theory*, translated by P. J. Shepard (Pergamon, New York, 1971).
[28]M. S. Child, *Molecular Collision Theory* (Academic, New York, 1974).
[29]L. D. Landau and E. M. Lifshitz, *Mechanics* (Addison-Wesley, Reading, 1969).
[30]R. Böttner, U. Ross, and J. Peter Toennies, J. Chem. Phys. **65**, 733 (1976).
[31]W. Eastes, U. Ross, and J. Peter Toennies, Chem. Phys. **39**, 407 (1979).
[32]L. Landau and E. Teller, Phys. Z. **10**, 34 (1936).
[33]R. N. Schwartz, Z. I. Slawsky, and K. F. Herzfeld, J. Chem. Phys. **20**, 1591 (1952).
[34]M. S. Chou, F. F. Crim, and G. A. Fisk, Chem. Phys. Lett. **20**, 464, (1974).

[35]Philipp *et al.* (Ref. 12) have studied the collisions of Li^+ with $N_2(v)$, $v \leq 3$ and $j = 0$, at a relative translational energy of 2 eV using the IA and conclude the following: "The important result is that there is considerable energy transfer between translational and vibro-rotational degrees of freedom, but no transfer from vibration to rotation." These authors define energy transfer as

$$\bar{\Delta}\varepsilon = \left| \sum_{v',j'} \Delta\varepsilon \frac{d\sigma}{d\Omega}(v'j' \leftarrow v0) \right| \Big/ \left| \sum_{v',j'} \frac{d\sigma}{d\Omega}(v'j' \leftarrow v0) \right| ,$$

a quantity one would more reasonably call the *average* energy transfer. It is clear from their Fig. 1 that for $v > 0$ and $\Delta\varepsilon < 0$, i.e., when translational energy increases, rotational resonances corresponding to V to R energy transfer are observed. Further, as v increases, these resonances become broader, indicating that a larger amount of energy is being transferred from V to R. There is a great deal of cancellation between the positive and negative components of $\bar{\Delta}\varepsilon$, with the result being that the average energy transfer is independent of v. The conclusion then should have been as follows: Although a great deal of energy may be transferred between vibration and rotation in individual collisions, *on the average*, in hyperthermal collisions, no energy is transferred from vibration to rotation. For thermal collisions involving a highly excited vibrationally and/or rotationally excited molecule, this conclusion may not hold because of the lack of energy transfer from translational to internal degrees of freedom. That the rotational energy can also be converted into vibrational energy may easily be seen from Fig. 5 of Philipp, Korsch, and Eckelt (PKE). The top panel shows a plot of a differential cross section at a scattering angle of 90° for a N_2-Li^+ collision as a function of the final state of the molecule, the initial state being $j = 34$ and $v = 0$. The threshold for exciting the $v = 2$ level is seen to be lowered from 0.584 eV to about 0.35 eV, showing that nearly 0.23 eV out of 0.30 eV of R energy is converted into V energy.